This article has been accepted for publication in a future issue of this journal, but has not been fully edited. Content may change prior to final publication. Citation information: DOI 10.1109/TII.2019.2895066, IEEE Transactions on Industrial Informatics



# New ARMO-based MPPT Technique to Minimize Tracking Time and Fluctuation at Output of PV Systems under Rapidly Changing Shading Conditions

Mehdi Seyedmahmoudian, *Member, IEEE,* Tey Kok Soon, *Member, IEEE,* Ben Horan, Alireza Safdari Ghandhari, Saad Mekhilef, *Senior Member, IEEE and Alex Stojcevski, Member, IEEE*

***Abstract*—The presence of bypass diodes that mitigate the negative effects of partial shading (PS) conditions produces multiple peak characteristics at the output of a photovoltaic (PV) array. Conventional maximum power point tracking (MPPT) methods develop errors under certain circumstances and detect the local maximum power point (LMPP) instead of the global maximum power point (GMPP). Several artificial intelligence (AI)-based methods have been used to modify the performance of conventional controllers. However, these methods have either not completely solved the PS problem or resulted in considerably complicated and unreliable methodologies, as well as require further development to be used in high-speed applications. This study aims to design, develop, and verify a novel rapid, reliable, and cost-effective method called adaptive radial movement optimization (ARMO) to diminish the effect of the PS problem in the MPP detection for PV systems with additional dynamic applications. The main advantages of ARMO are its improved tracking speed and a significant reduction in output fluctuations during the tracking period. An extensive experimental verification has been conducted to provide a fair evaluation of the proposed method compared with conventional and recently developed methods under similar conditions while being applied to a unique PV system and DC/DC converter.**

***Index Terms*—Photovoltaic System, Maximum Power Point Tracking, Partial Shading, Energy Conversion, Metaheuristic Optimization**

## I. INTRODUCTION

Photovoltaic (PV) systems are currently among the rapidly emerging technologies due to their clear, quiet, and low-maintenance characteristics. However, this on-demand source of energy suffers from relatively low output efficiency compared with other alternatives. One of the considerable challenges that affect the efficiency of PV systems is the partial shading (PS) condition because these systems must be installed outdoors. This issue is often resolved by inclusion of a bypass diode to a specific number of cells in the series circuit. However, the presence of bypass diodes in the series-connected modules results in multiple peaks at the output of the PV system. This result significantly reduces the efficiency of conventional techniques, such as the perturb and observe (P&O) and hill climbing (HC) approaches [1-3], and some recently developed techniques [4, 5], in extracting the maximum power at the output of a PV array.

Several studies [6, 7] on soft computing methods, such as fuzzy logic controller (FLC) and artificial neural networks (ANNs), have been conducted. A few of these studies have used FLC to increase the efficiency and reliability of the maximum power point (MPP) tracking controller under normal conditions. For instance, authors in [8], used FLC to increase the efficiency and speed of the HC method during the tracking process. In this study, FLC was used to scan and store the MPP region in the first stage, and then HC is used to track the actual MPP in the second stage. In another study, a combination of FLC and ANN was proposed to track the global maximum power point (GMPP) of a PV system using the cell temperature and irradiance level in the ANN training process [6]. These studies used varied approaches to achieve a satisfactory performance in determining GMPP under normal and several PS conditions. However, these approaches are limited because they are computationally heavy with respect to the fuzzification, rule base, defuzzification, and training procedures [9, 10].

Several evolution-based techniques, such as differential evolution (DE), genetic algorithm (GA), simulated annealing (SA), firework algorithm (FWA), and particle swarm optimization (PSO), have been used to identify the GMPP among several local maximum power points (LMPPs) at the output of partially shaded PV system [11-16]. PSO is one of the most popular techniques in the literature [11,12, 16] because of its capabilities in targeting stochastic functions. However, the standard format of this method has several drawbacks, such as constant particle velocity, high dependency on random coefficients, long tracking time due to low convergence speed, and high computational cost because the large memory must record particle movement in microcontrollers. Several studies have attempted to address these issues by modifying the performance of the standard PSO. However, a few drawbacks remain even in the modified versions. In one study, a deterministic PSO method associated with random coefficients that have been removed was used to decrease the metaheuristic aspect of evolutionary algorithms [17]. In other studies, PSO in the form of a hybrid technique was used with other methods to

Manuscript received August 08, 2018, revised November 21, 2018; accepted January 09, 2018. Date of publication ??; date of current version ??. M. Seyedmahmoudian, and A. Stocevski are with the School of Software and Electrical Engineering, Swinburne University of Technology, Melbourne, Australia (e-mail: mseyedmahmoudian@swin.edu.au; astojcevski@swin.edu.au). B. Horan is with the School of Engineering, Deakin University, Geelong, Australia (e-mail: ben.horan@deakin.edu.au). T. K. Soon, is with Department of Computer System & Technology, Faculty of Computer Science & Information Technology, University of Malaya, Malaysia. (e-mail: koksoon@um.edu.my). S. Mekhilef, and A. S. Ghandhari are with the Department of Electrical Engineering, University of Malaya, Malaysia (e-mail: Saad@um.edu.my).

1551-3203 (c) 2018 IEEE. Personal use is permitted, but republication/redistribution requires IEEE permission. See http://www.ieee.org/publications_standards/publications/rights/index.html for more information.

This article has been accepted for publication in a future issue of this journal, but has not been fully edited. Content may change prior to final publication. Citation information: DOI 10.1109/TII.2019.2895066, IEEE Transactions on Industrial Informatics



increase the accuracy and decrease the adverse effects of random coefficients [18-20]. However, these methods would result in considerably long processing time and high level of complexity [21-23].

This study aims to outline a unique, simple, and rapid metaheuristic soft computing method called adaptive radial movement optimization (ARMO) to detect GMPP under various PS conditions while the convergence speed and output fluctuations are minimized during the tracking period. ARMO is highly efficient in optimizing continuous search space. Compared with conventional methods, ARMO enables the MPPT control unit to track GMPP under PS conditions. The main benefit of ARMO is its considerably high level of efficiency and reliability under PS conditions with respect to speed, simplicity, and stability while tracking steady-state operations. These characteristics are in stark contrast to other metaheuristic approaches, such as the standard PSO and modified PSO (MPSO) methods presented in [19]. ARMO is also less reliant on random coefficients, requires less memory for processing, and creates less computational burden within the processing time. Therefore, a low-cost controller can be employed in the system. The proposed ARMO only requires the setting of two coefficients, and this optimization requires less memory and easy computation compared with the PSO algorithms which need setting of two coefficients and two random coefficients.

The rest of this paper is organized as follows. Section II briefly describes the problems associated with PS conditions in PV systems. Section III presents the theory and background of the proposed ARMO method, as well as the implementation of this method in the GMPP tracking unit of PV systems. Section IV provides the experimental implementation of the proposed ARMO–MPPT method and presents a comprehensive analytical comparison among several MPPT techniques under various static and moving PS conditions. Finally, Section V presents the discussion and conclusion of this study.

## II. PV System Under Partial Shading Conditions

A non-uniform shading condition occurs under any circumstances in which part of the PV system is affected by shadows. This condition is unavoidable for PV systems, particularly those in residential areas that are often affected by unpredictable shadows of buildings, passing clouds, trees, or even flying birds. Under these conditions, the ability to generate power differs between shaded and unshaded fractions of the PV system. This non-uniformly distributed irradiance level (i.e., PS condition) forces unshaded modules or sub-modules to operate in the reverse bias region to provide the same current as unshaded cells because of the constant current flow through every module in a series configuration (see Fig. 1). The operation of a PV cell in the reverse bias region can cause a hotspot in a PV system, thereby damaging the exposed cells in the reverse bias region and can ultimately cause an open circuit condition for the entire PV system. To avoid this disruptive consequence and overcome the hotspot phenomenon, bypass diodes have been introduced into the structure of PV modules. In Fig. 1 (a), two PV modules, with each module connected to a single bypass diode, experience PS. The associated characteristics of this system show how bypass diodes prevent the PV cells from falling into the reverse bias region.

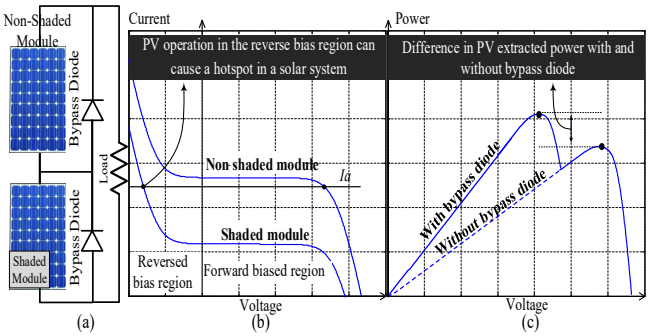


Fig. 1. Characteristics of a PV system with and without bypass diodes

Despite the significant benefits of adding bypass diodes to the PV modules, these diodes increase the complexity of extracting maximum power from the system. The characteristics of PV systems with and without bypass diodes are different. Under PS, where various fractions of PV systems receive different illumination levels, the diodes bypass the shaded modules, while the unshaded modules generate current in the string. Under PS conditions, the PV system embedded with bypass diodes creates multiple peaks at the output characteristics (see Fig. 1). The peak with the highest power value is called GMPP and the lower values are LMPP. The locations of the peak and patterns of PS have an unpredictable nature. Thus, setting the operating point of the converter on the maximum point is substantially complicated for the control unit. Recent studies have discussed the effects of PS on the efficiency of PV systems [24]. Multiple peaks on the PV curve are problematic for the majority of the MPPT approaches because the HC techniques may be limited to identifying the local MPP. Accordingly, the current study develops a novel ARMO method to efficiently track GMPP under different PS conditions.

## III. Adaptive Radial Movement Optimization

### *A) Theory*

A radial movement optimization is an optimization approach that is swarm-based and substantially similar to other evolutionary optimization approaches, such as PSO and DE [25]. The operational process of ARMO is considerably similar to the RMO method. However, the coefficients in ARMO adaptively change throughout the algorithm process. ARMO begins the optimization process by scattering multiple particles in the predefined search space. Then, the scattered particles are considered as proposed solutions and the fitness values of all particles are calculated using the objective function at each step of the optimization process. A movement vector is determined by a random vector and the best two fitness values. The main difference between ARMO and other optimization methods is the movement style of the particles. In this technique, the particles explore the defined area around the center. In Fig. 2, the particles move out with different velocities along the radii around the center. The location of the best particle is identified based on their fitness values, which are defined by the objective function. This radial movement approach particles to explore the search space efficiently and avoid falling out of the search

1551-3203 (c) 2018 IEEE. Personal use is permitted, but republication/redistribution requires IEEE permission. See http://www.ieee.org/publications_standards/publications/rights/index.html for more information.

This article has been accepted for publication in a future issue of this journal, but has not been fully edited. Content may change prior to final publication. Citation information: DOI 10.1109/TII.2019.2895066, IEEE Transactions on Industrial Informatics



space or converging toward the local optima. This phenomenon provides a better and denser exploration around the target point in the search space.

One of the major issues for existing techniques, such as PSO, MPSO and ACO, is the long and expensive computation time. Therefore, the majority of these methods perform well in small or medium search spaces because, in many of these techniques, the locations and velocities of all particles need to transfer across the iterations. However, in the proposed ARMO, the particles start moving from an updated point in every iteration step, and the location and velocity of all particles are not stored and transferred between different iterations. Therefore, this technique is more suitable for large and complex search spaces and requires less memory throughout its exploration. Meanwhile, the existence of a global best vector in the updating process prevents the algorithm from being trapped in local optima. Similar to DE and PSO, the particle location within the search space is represented by a matrix of size *nop* × *nod*. *nop*, which represents the number of particles used as specified by the designer. In particular, *nod* represents the number of dimensions, which is dependent on the number of variables required to be optimized. Particle locations are determined by the following matrix; for each trial, *nop* and *nod* remain constant. The stages of the optimization approach are detailed in the following subsections.

$$X_{i,j}=\begin{bmatrix} X_{1,1} & X_{1,2} & \cdots & X_{1,nod} \\ X_{2,1} & \ddots & \cdots & \vdots \\ \vdots & \vdots & \ddots & \vdots \\ X_{nop,1} & X_{nop,2} & \cdots & X_{nop,nod} \end{bmatrix} \quad where \begin{cases} i=1,2,3,\ldots,nop \\ j=1,2,3,\ldots,nod \end{cases} \tag{1}$$

*1) Initialization*

Initial particle locations are randomly assigned within the boundaries of the search space. An example of this random assignment is as follows:

$$X_{i,j}=X_{\min(j)}+rand(0,1)\times\left(X_{\max(j)}-X_{\min(j)}\right)$$
$$where\begin{cases} i=1,2,3,\ldots,nop \\ j=1,2,3,\ldots,nod \end{cases} \tag{2}$$

where $X_{max(j)}$ and $X_{min(j)}$ denote the *j*th dimension constraints specified by the designer of the system, and a normal distribution, such as Gaussian distribution between 0 and 1, is used for Rand (0,1).

*2) Movement Vectors*

The particles spread in straight line paths from the center along the radii based on the vector $V_{i,j}$ obtained from the following equation:

$$V_{i,j}=rand(0,1)\times V_{\max(j)}$$
$$where\quad \begin{cases} V_{\max(j)}=\dfrac{X_{\max(j)}-X_{\min(j)}}{k} \\ i=1,2,\ldots,nop;\ j=1,2,\ldots,nod \end{cases} \tag{3}$$

where *k* is a positive integer and equals to 2 in this study. In the aforementioned approaches, which rely on particles to search the search space, an inertia weight is used to address issues with convergence. In the radial movement optimization, the inertia weight is denoted by *W* and reduced based on the number of iterations. The relationship between the iteration number and inertia weight *W* is shown by Eq. (5).

$$V^{k}{}_{i,j}=W_k\times rand(0,1)\times V_{\max(j)} \tag{4}$$

In ARMO, the value of $W_k$ is a constant value in the range of 0–1 for the first 10 iterations and will be adjusted based on Eq. (5) for the rest of the iterations.

$$W_k=W_{\max}-\frac{W_{\max}-W_{\min}}{Iteration_{\max}}\times 2\times Iteration_k, \tag{5}$$

where $W_{max}$ was specified as 1 and $W_{min}$ as 0, $iteration_k$ is the current iteration, and $iteration_{max}$ is the maximum number of iterations, which is 30 in this study. The radial movement of particles from the center is depicted in Fig. 2 and calculated by (6).

$$X^{k}{}_{i,j}=Centre^{k}+V^{k}{}_{i,j} \tag{6}$$

The particles are shown as black dots scattered from the center, and the boundaries of $V_{max}$ are shown as a dashed circle.

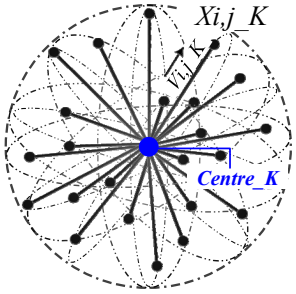


Fig. 2. Exploration of particles in search space along the radii

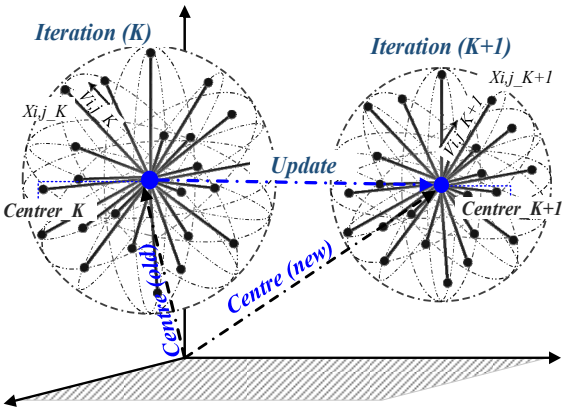


Fig. 3. Center point updating process in two consecutive iterations

Unlike in DE and PSO, the particles do not travel throughout the solution space, thereby eliminating the need to save all current particle locations for the next step. After the particles have been scattered, the objective function is used to score the fitness of the particles and define the radial best (R*best*), which is the particle with the best fitness value. This location and its fitness value are saved in this step. Another best value is the global best (G*best*), which is the location of the R*best* that has been explored in all steps. R*best* and G*best* are used to incrementally update the center using the following equation:

$$Centre^{new}=Centre^{old}+C_1\times\left(Gbest-Centre^{old}\right)+C_2\times\left(Rbest-Centre^{old}\right) \tag{7}$$

where $C_1$and $C_2$ are coefficients calculated by Eq. (9) and Eq. (10) after the optimization process begins. After the location of the center point is updated, particles are re-scattered from the new location of the center. Then, *Gbest* is compared with *Rbest.*

1551-3203 (c) 2018 IEEE. Personal use is permitted, but republication/redistribution requires IEEE permission. See http://www.ieee.org/publications_standards/publications/rights/index.html for more information.

This article has been accepted for publication in a future issue of this journal, but has not been fully edited. Content may change prior to final publication. Citation information: DOI 10.1109/TII.2019.2895066, IEEE Transactions on Industrial Informatics



In a case where *Rbest* indicates a fitter solution, *Gbest* is updated by the current location of *Rbest*. In general, at each iteration step, the objective function returns a fitness value for each particle. The location of the best fitness value is stored as the best radial solution, *Rbest*, and the best *Rbest* experienced by the algorithm, so far, is called *Gbest*. Thus, *Rbest* is the best solution obtained among all the evaluated particles at each generation, and *Gbest* is the best solution ever obtained among all generations. This process continues until *Gbest* equals a threshold value or until the iteration number equals a maximum value. Fig. 3 depicts two successive iterations where the update vector specifies a new center.

### *B. ARMO-based MPPT*

The maximum borders for the radii are constant in the standard radial movement optimization [26]. However, these borders change throughout the algorithm operation in the ARMO method. This adaptive change in search space borders in each iteration results in a smooth and rapid convergence in the proposed MPPT unit. The ARMO-based MPPT technique considers the search space as a vector comprised of converter operational duty cycles that correspond to different voltages at the output terminals of the PV system. As shown in Eq. (8), this vector represents the locations of $N$ participating particles in the search space. In fact, each location refers to a duty cycle value that can be the potential GMPP for the connected PV system. Each particle has its own fitness value, which is determined on the basis of generated power at the output terminal of the PV system.

$$X_i^k = \left[ X_1^k, \quad X_2^k, \quad \dots \quad \dots \quad , X_i^k, \quad , \dots\dots, \quad X_{N-1}^k, \quad X_N^k \right] \quad (8)$$

#### *1) Selection of ARMO Coefficients*

The ARMO method has two variable coefficients denoted by $C_1$ and $C_2$. These coefficients directly influence $G_{best}$ and $R_{best}$ by contributing a certain level of flexibility at a required level of optimization and affects the convergence of the algorithm toward the GMPP. In general, the two coefficients can affect the exploration trajectory of the particles and convergence speed of the ARMO technique by biasing the direction of the center point throughout different iterations. In contrast to the original RMO, in the proposed ARMO technique, the values of these coefficients change during the algorithm process. In general, $C_1$ and $C_2$ can be chosen in a range of 0.9–0.4, where the higher values for $C_1$ increase the pace of convergence. However, an excessively large value for this coefficient (over 0.9) decreases the convergence quality of the technique. The larger $C_1$ compared with $C_2$ would bias sampling toward the direction of $G_{best}$, while larger $C_2$ compared with $C_1$, guides the algorithm toward the direction of *Rbest*. In the proposed ARMO method, the values of $C_1$ and $C_2$ are adapted throughout the iterations using the following equations:

$$C_{1k} = C_{1\min} + \frac{C_{1\max} - C_{1\min}}{Iteration_{\max}} \times Iteration_k \quad (9)$$

$$C_{2k} = C_{2\max} - \frac{C_{2\max} - C_{2\min}}{Iteration_{\max}} \times Iteration_k \quad (10)$$

The length of the update vectors would increase if the values of $C_1$ and $C_2$ exceeded 1. This result slows the convergence and reduces the ability of the algorithm to determine the global optimum point [25]. In this study, the maximum and minimum values for $C_2$ and $C_1$ are 0.9 and 0.4, respectively. In addition, in the proposed ARMO technique, the value of inertia weight ($W_k$) decreases twice faster than the way that has been considered in the original RMO. Furthermore, the value of this coefficient remains constant for the first 10 iterations, thereby allowing particles to explore the larger sections of the search space in the early stage where the region for GMPP is not yet identified. This faster decrease in the following iteration helps the particles converge toward the actual GMPP at the final iterations when the global region is identified.

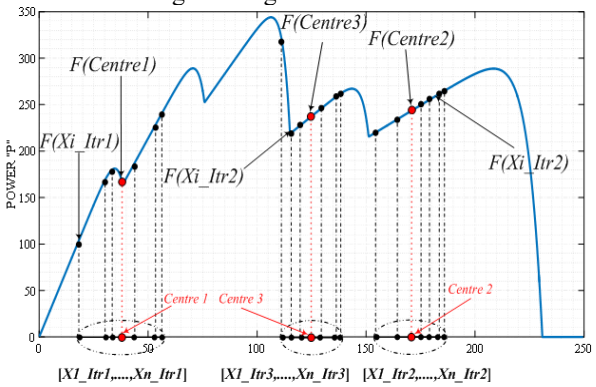


Fig. 4. Movement of particles in ARMO–MPPT technique

To demonstrate the procedure of the ARMO technique in the MPPT application, a simplified illustration of the particle movements across three consecutive iterations are shown in Fig. 4. This figure shows the locations of the particles on the P–V characteristic curve of the PV system. As shown in Fig. 4, in the first iteration (on the left side of the figure), the larger section of the search space is explored, and the best fitness (power value) in this region is obtained by the algorithm. In the next iteration (on the right side of the figure), the radii of the circle are slightly decreased. Therefore, a slightly smaller section of the search space is explored, and the best fitness is obtained in this section, in the third iteration (on the right side of the figure). Again, the previous center locations and values of Rbest and $G_{best}$ identify the location of the new center in the current iteration. Then, the new center location is calculated, and the particles search for the best fitness location around the radii. Once the best radial solution is obtained, it is compared with the $G_{best}$ value and updates it if an improvement occurs. This process continues for all iterations until the global maximum power region is identified and particles converge into the actual GMPP. In the final iterations, the centers and selected regions are very close to one another. In a real-world implementation, instantaneous variations in the levels of solar irradiance during PS can cause fluctuations in the generated power. Accordingly, Eq. (11) is designed in the proposed method to initialize the MPPT controller and track the new GMPP when the magnitude of the variation is more than the minimum allowable power variation at the output power of the PV system. This condition is given by $\Delta P$ as follows:

$$\left| \frac{F(X_{i+1}) - F(X_i)}{F(X_i)} \right| > \Delta P, \quad (11)$$

where $F(X_i)$ represents the power output by the solar panel based on the $i$th particle location $X_i$ in the search space. PS is a natural phenomenon; thus, it is stochastic. Moreover, any

1551-3203 (c) 2018 IEEE. Personal use is permitted, but republication/redistribution requires IEEE permission. See http://www.ieee.org/publications_standards/publications/rights/index.html for more information.

This article has been accepted for publication in a future issue of this journal, but has not been fully edited. Content may change prior to final publication. Citation information: DOI 10.1109/TII.2019.2895066, IEEE Transactions on Industrial Informatics



number of PS conditions is possible. In this study, the threshold (ΔP) is 1% of the PV power at the maximum point.

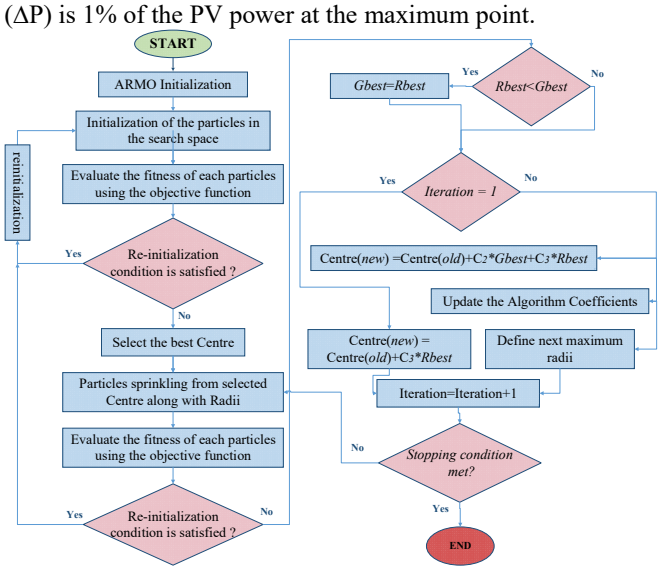


Fig. 5. Flowchart of ARMO technique

## IV. Experimental Implementation and Results

### A. Experimental Setup

A comprehensive experimental implementation was performed to verify the performance of the proposed ARMO–MPPT controller under various PS conditions. The experimental setup was employed to compare the performance of the proposed ARMO method with the improved PSO, standard PSO, and conventional incremental conductance (InC) methods. In this study, the selected values for standard and modified PSO are based on the values used in [11, 12, and 19]. The developed experimental test bench included the PV simulator to create different PS conditions and environmental changes, a reliable DC-DC converter associated with the sensors and gate drives, and a microcontroller to provide the output pulse width modulation (PWM) signals based on the final command of the control algorithm. To cover a wide range of PS conditions (i.e., from the minor to the most crucial), the Chroma 6200 series PV simulator was used to create several PS scenarios. An array consisting of six KC85T PV series-connected modules was designed in the Chroma Soft Panel software and operated under various testing conditions. The block diagram and experimental setup of the prepared MPPT system are shown in Fig. 6. The Chroma PV simulator provided the input power for the designed DC-DC converter, which was connected to the load (see Fig. 6). This study selected a single-ended primary-inductor converter (SEPIC) as the DC-DC converter in the experimental implementations. SEPIC has the ability to step up and step down the output voltages. It only has operational regions and is able to operate in all regions of the I–V curve. In addition, the output voltage of the converter is non-inverted; thus, the input-output polarities of the converter are equal and the ground on both sides can be shared. The specifications and selected components of the designed SEPIC converter are as follows: Cin and Cout = 3900 uF, L1 and L2 = 250 uH, Cs = 1000 uF, and the load is a 10-Ω resistor. The switching frequency for the selected IGBT is set to 20 kHz and the sampling time for the system is 50 ms. The operating voltage and current were measured and transferred to the controller through the connected voltage and current transducers, which are LEM 25-P and LEM LA 25-NP, respectively. The measured operating voltage and current were sent to an Atmega 328P microcontroller that was embedded with a 10-bit analogue-to-digital converter. The measured signals were used in the MPP tracking process in the microcontroller, which was compiled with the proposed MPPT method. During the tracking period and upon completion, the required PWM signal was sent to the IGBT switch in the converter through the associated gate drive circuit. A gate drive with a signal frequency of 20 kHz was designed to switch the converter, which regulated the output voltage and tracked the MPP. The gate drive circuit ensured that the PWM signal was noise free and its level was compatible with the required signal by the gate to switch on IGBT.

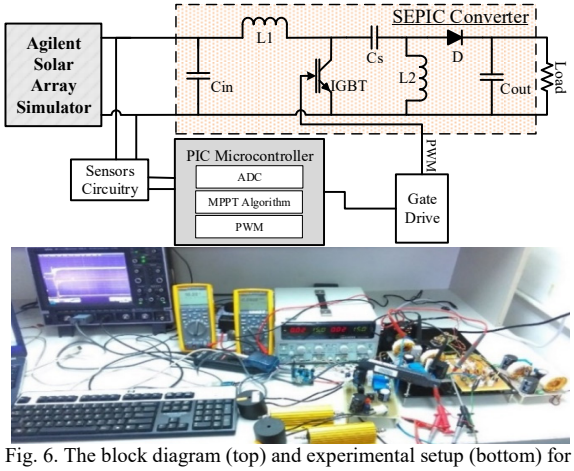


Fig. 6. The block diagram (top) and experimental setup (bottom) for the proposed ARMO based MPPT technique

### B. Shading Scenarios

Different mismatching conditions, such as PS conditions, moving shadows, rapidly changing irradiance levels, and sudden changes in output loads, were created in the experimental implementation of this study to verify the performance of the proposed method under any PS condition. In the rest of this section, the design of the PS conditions is first explained, and then the performance of the proposed MPPT technique is evaluated and compared with that of the other techniques under different mismatching conditions. To fairly compare and reveal the performance of the proposed MPPT techniques, all parameters, including number of particles, stopping conditions, and number of iterations, were designed equally for all the participating MPPT techniques. The PSO and MPSO parameters are set as C1 = 1.2, C2 = 1.6, W = 0.4 in this study [11,12, 19].

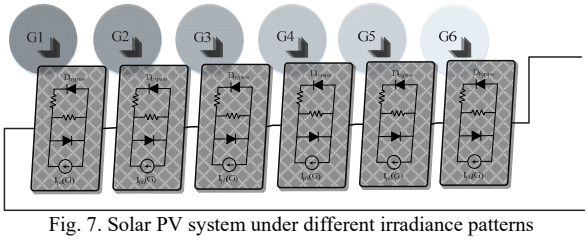


Fig. 7. Solar PV system under different irradiance patterns

#### 1) Shading Scenario 1

In this scenario, the six modules (i.e., G1 to G6) presented in Fig. 7 received solar irradiance of 1000, 1000, 1000, 800, 600, and 500 W/m$^2$. Under this condition, GMPP occurs as the first

1551-3203 (c) 2018 IEEE. Personal use is permitted, but republication/redistribution requires IEEE permission. See http://www.ieee.org/publications_standards/publications/rights/index.html for more information.

This article has been accepted for publication in a future issue of this journal, but has not been fully edited. Content may change prior to final publication. Citation information: DOI 10.1109/TII.2019.2895066, IEEE Transactions on Industrial Informatics



peak among the four peaks that appear at the output of the PV system. The output P–V characteristics of the PV system under these conditions and the output performances of the different MPPT controllers are shown in Figs. 8 to 10.

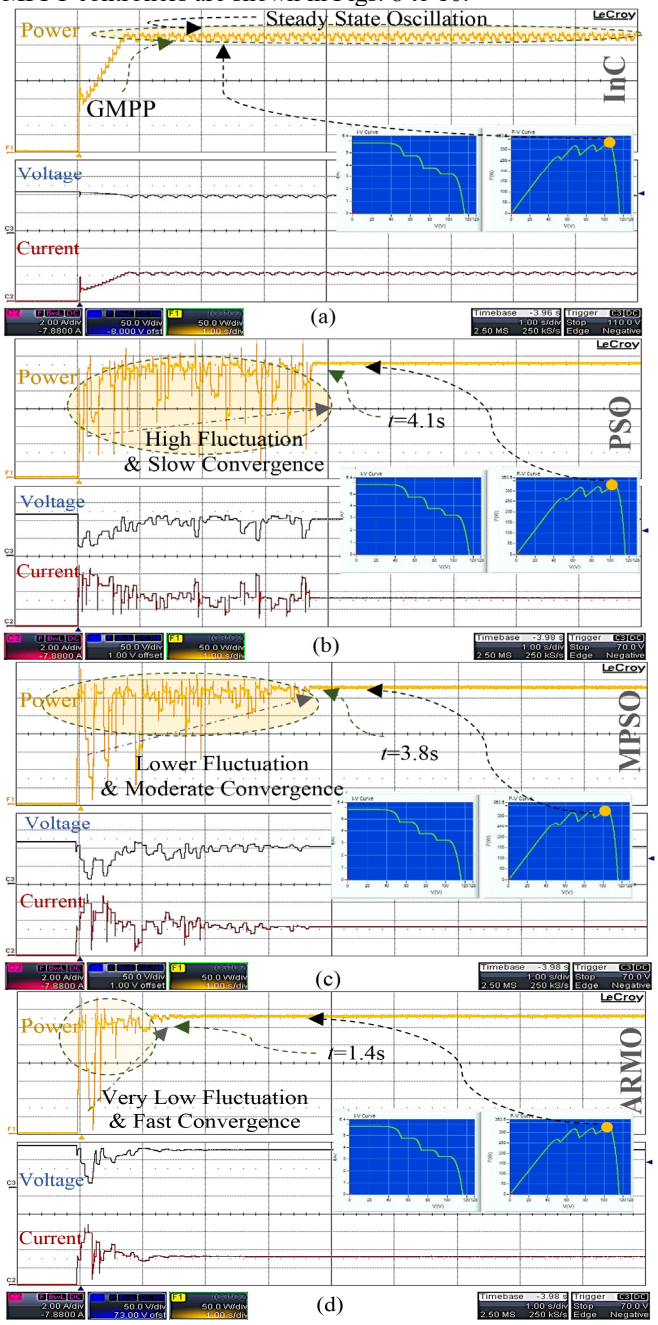


Fig. 8. Experimental comparison of different MPPT techniques under shading scenario 1: (a) InC, (b) PSO, (c) MPSO, and (d) ARMO methods

The results show that the conventional InC–MPPT successfully tracks the GMPP in a short time. If this first point is LMPP, then the algorithm stops in that location. However, if the first point is GMPP, then the algorithm has unintentionally determined the actual GMPP. Therefore, the PV systems have low efficiency when the conventional MPPT techniques are used. By contrast, the performance of the other MPPT methods in this study confirms that the metaheuristic approach searches the entire range of the search space before finalizing the output signals that determine the steady-state operating point of the converter. Thus, regardless of the GMPP position at the output characteristics of the PV system, a reliable and system-independent method must evaluate the search space within the initial iterations. However, the manner by which the algorithm explores the search space defines the superiority of one method over the others. Nearly all tested metaheuristic-based MPPT systems satisfied the requirement of determining GMPP under PS conditions. However, convergence speed, output fluctuation, complexity, and total tracking time, among others, are the factors that must be compared with the new iteration of MPPT control techniques. The results also showed that the standard PSO technique can track GMPP but at the cost of long tracking time and numerous large fluctuations at the output of the PV system. Therefore, the MPSO-based MPPT control method outperforms the standard PSO method because the fluctuation levels were significantly reduced, and the particles began converging toward the GMPP after the initial explorations. However, the output results of the proposed ARMO technique showed that this MPPT control scheme performs better than the other two MPPT methods with respect to convergence speed, output fluctuations, and total tracking time. Fig. 8 shows that the ARMO–MPPT controller tracks GMPP in as short as 1.4 s, which is significantly less than the tracking time for the PSO and MPSO methods, which are 4.1 s and 3.8 s, respectively. This result also shows that the quantity and magnitude of fluctuations during the tracking period were reduced when the ARMO technique was used.

*2) Shading Scenario 2*

The second shading scenario represents environmental conditions in which the six modules (i.e., G1 to G6) in the designed PV array received solar irradiance of 500, 300, 150, 0, 1000, and 1000 W/m$^2$. Under these PS conditions, four peaks appear at the output PV characteristic, in which the GMPP occurs as the last peak where the power is approximately 178.2 W (see Fig. 9). Under this condition, SEPIC operates with a duty cycle near 1. The performance of the conventional InC method under this condition shows that this technique fails to track GMPP (180 W) at the output of the PV system, and instead tracks the first peak (100 W) that occurs in the initial part of the duty cycle search space. Evidently, this technique is characterized by steady-state oscillations around MPP, which can be signified because the generated power of the PV system is increased. This condition is mainly due to the operating point that constantly oscillates around MPP until the output characteristic changes using the InC method when MPP is determined. The output results of the standard and modified PSO and the proposed ARMO methods show that these algorithms can track GMPP at the output characteristic of the PV system (see Figs. 9 (a) to (d)). Although the convergence speed of the MPSO method is significantly faster than that of the standard PSO method, the tracking speed of the former is significantly longer than the proposed ARMO technique. PSO and MPSO tracked GMPP within approximately 3.8 s and at approximately 1.2 s when ARMO–MPPT is applied. In addition, limited oscillations are presented at the output terminal when ARMO is employed in the MPP tracking unit.

*3) Shading Scenario 3*

Under the third PS condition, the six PV modules (i.e., G1 to G6) in the array receive solar irradiance of 800, 600, 500, 300, 150, and 100 W/m$^2$, which resulted in a P–V characteristic with five MPPs (see Fig. 10). This figure shows that GMPP occurs

1551-3203 (c) 2018 IEEE. Personal use is permitted, but republication/redistribution requires IEEE permission. See http://www.ieee.org/publications_standards/publications/rights/index.html for more information.

This article has been accepted for publication in a future issue of this journal, but has not been fully edited. Content may change prior to final publication. Citation information: DOI 10.1109/TII.2019.2895066, IEEE Transactions on Industrial Informatics



in the middle of multiple LMPPs. Thus, conventional techniques cannot easily track the actual MPP of the PV system under this condition. The performances of the proposed ARMO, MPSO, standard PSO and conventional InC methods are shown in Figs. 10 (a) to (d), respectively. Under this condition, the conventional MPP techniques cannot track the GMPP because it occurs in the middle of multiple LMPP tracks instead of in the GMPP. Although no significant fluctuation occurred during the tracking period, the constant oscillation remains at the output of the system even in the steady-state operation mode. The modified PSO method has considerably mitigated the problems associated with the standard PSO, particularly the massive fluctuations at the output characteristic (see Fig. 10 (c)). However, its performance is not highly satisfactory, and the tracking period remains lengthy.

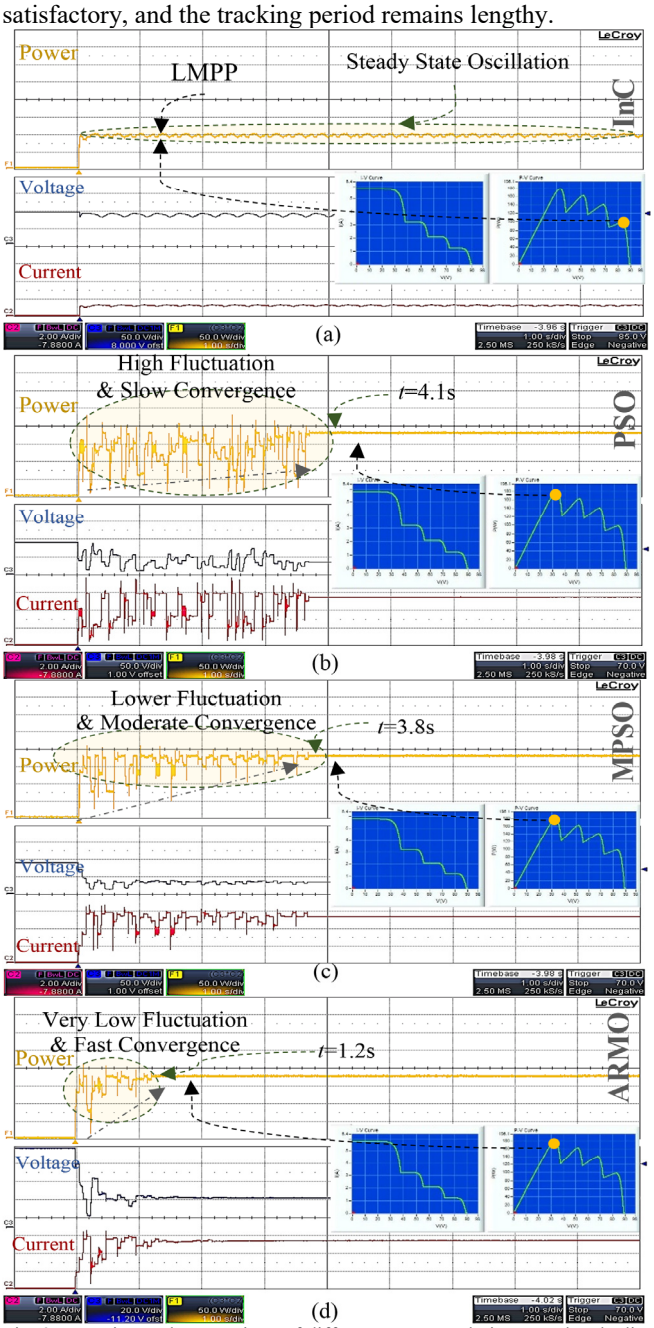


Fig. 9. Experimental comparison of different MPPT techniques under shading scenario 2: (a) InC, (b) PSO, (c) MPSO, and (d) ARMO methods

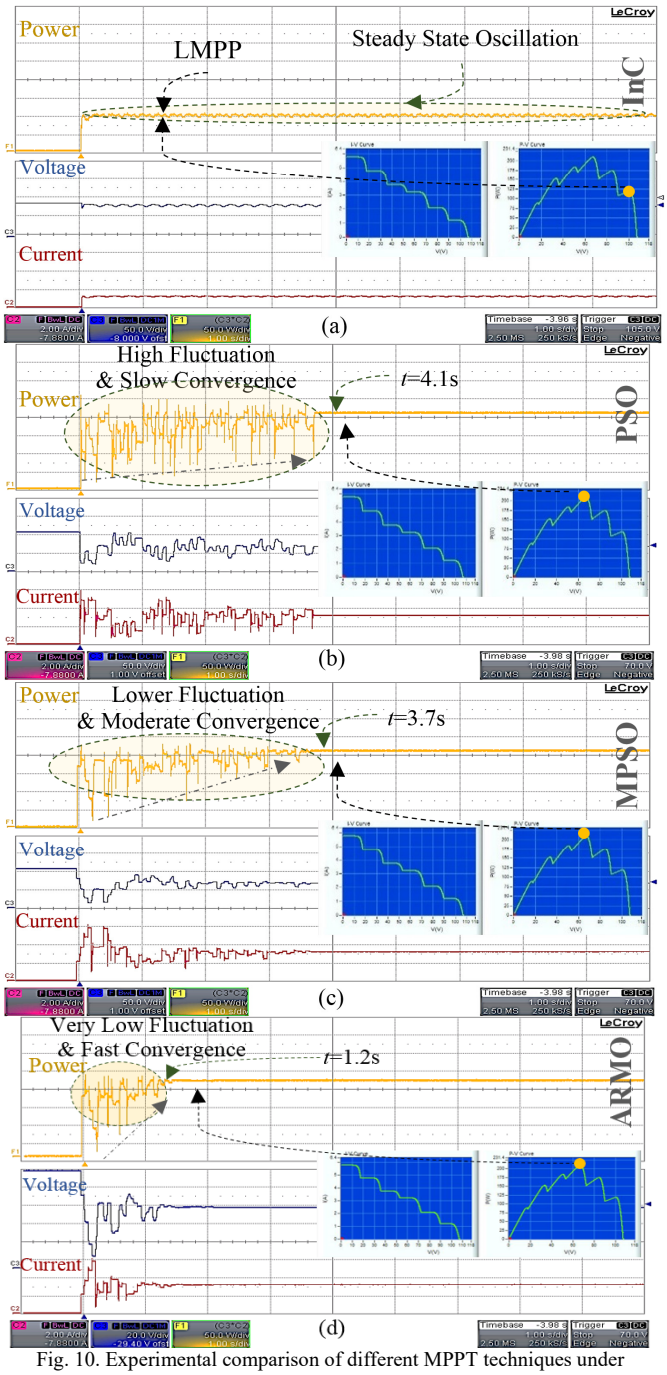


Fig. 10. Experimental comparison of different MPPT techniques under shading scenario 3: (a) InC, (b) PSO, (c) MPSO, and (d) ARMO methods

Fig. 10 (d) shows how the proposed ARMO-based technique tracks the GMPP at the output of the PV system under the third shading scenario. The entire tracking process consumes approximately 1.2 s, which is extremely rapid compared with the tracking time of the PSO and MPSO methods, which are 4.1 s and 3.7 s, respectively. In addition, the output fluctuation is significantly reduced when the ARMO-based MPPT is used.

*4) Shading Scenario 4*

To further evaluate the tracking accuracy of the proposed MPPT technique, the fourth scenario is designed to create the output characteristic in which the value of the GMPP is very

1551-3203 (c) 2018 IEEE. Personal use is permitted, but republication/redistribution requires IEEE permission. See http://www.ieee.org/publications_standards/publications/rights/index.html for more information.

This article has been accepted for publication in a future issue of this journal, but has not been fully edited. Content may change prior to final publication. Citation information: DOI 10.1109/TII.2019.2895066, IEEE Transactions on Industrial Informatics



close to the value of LMPPs. In this scenario, the six modules (i.e., G1 to G6) in the array receive solar irradiance of 1,000, 1000, 1000, 1000, 800, and 600 W/m$^2$. Under these PS conditions, a characteristic with three peaks appeared at the output of the PV system. Under these PS conditions, the difference between the value of the actual GMPP (middle peak) with the nearest LMPP is very small (~1.5%). Therefore, this scenario can be an important testing condition to evaluate the accuracy of the proposed algorithm. In the first experiment, given the simple P&O approach of this method, the first peak from the left is tracked as the final MPP of the system. As half of the PV modules receive full solar irradiance levels, the overall power generation under this condition is higher than the power levels of the PV system under previous shading scenarios. Therefore, the magnitude of steady-state oscillation, which is one of the disadvantages of the InC-based MPPT technique, is higher in the output power of the PV system under this condition compared with previous shading conditions. In Fig. 11 (a), the magnitude of these oscillations is as large as 20 W. The performance results of the standard and modified PSO are shown in Figs. 11 (b) and (c). Apart from the slow convergence, many disruptive fluctuations exist at the output of the PV system, which has a significant negative effect on the overall stability of the PV system. The tracing fluctuation under this condition is even more crucial because the difference between the GMPP and LMPP is negligible, and the PSO algorithm is unable to track the actual GMPP until the final stages of the algorithm. Examination of the output results for the ARMO method (see Fig. 11 (d)) indicates a significant improvement in the performance of the PV system during the tracking period when the ARMO–MPPT technique is used in the system. The output performance shows that the ARMO method finds the global region at approximately 0.5 s and then accurately tracks the GMPP from the LMPPs in less than 1.1 s. The tracking times for the PSO and MPSO are however 4.1 s and 3.8 s, respectively. The performance of the ARMO technique under this condition also shows that regardless of the shading pattern at the P–V characteristic, the PV system shows lower fluctuations during both steady-state and transient periods when the ARMO–MPPT is used.

Given the metaheuristic nature of the proposed ARMO technique and its system independency approach, no information on the PV characteristic is required. Therefore, the proposed system was evaluated several times, that is, 10 times in this study, to demonstrate its precision and system independence under various conditions. Table 1 shows the summary of these results. $P_M$ refers to the arithmetic mean value of the maximum ($P_{MMAX}$) and ($P_{MMIN}$) is the minimum measured power values among all 10 tests. The tracking power efficiency ($P_{EE}$), which is used to evaluate the results, is a part of the arithmetic mean value and actual global maximum power value tracked by the proposed algorithm under partial shading conditions ($P_{EE} = (P_M / P_A) \times 100$).

TABLE I. OUTPUT RESULTS OF ARMO ALGORITHM UNDER FOUR CONDITIONS

| Test condition | $P_A$ (exp) | $P_{Mmax}$ (ARMO) | $P_{Mmin}$ (ARMO) | $P_M$ (ARMO) | $P_{EE}$ (%) |
|---|---|---|---|---|---|
| Scenario 1 | **330.6** | **330.5** | **329.4** | **109.2** | ***99.8*** |
| Scenario 2 | **178.2** | **178.2** | **177.8** | **178.0** | ***99.8*** |
| Scenario 3 | **210.4** | **210.4** | **209.9** | **210.2** | ***99.9*** |
| Scenario 4 | **402.6** | **402.6** | **402.2** | **402.4** | ***99.9*** |

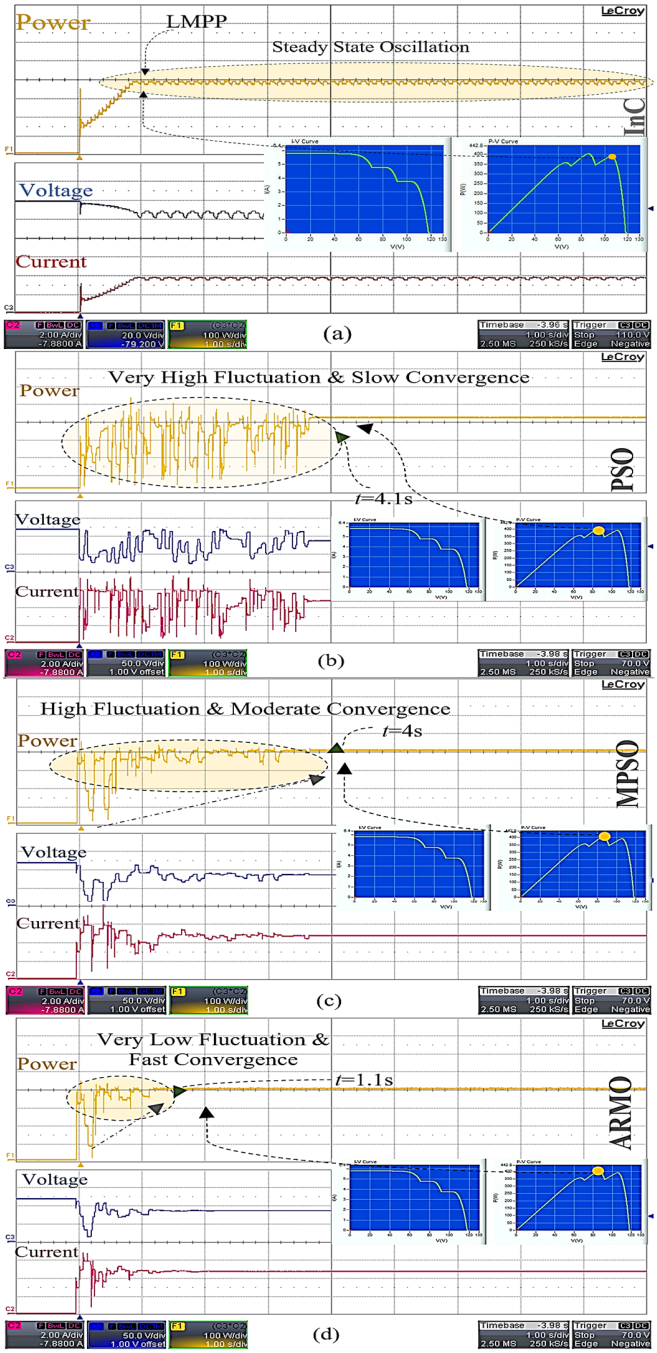


Fig. 11. Experimental comparison of various MPPT techniques under shading scenario 4: (a) InC, (b) PSO, (c) MPSO, and (d) ARMO methods

### C. Rapid Shadow Moving Condition

The positive effect of employing a rapid and reliable MPPT technique on the overall performance of the PV system is considerably significant when the system is evaluated under rapidly changing conditions. Under these conditions, a reliable MPPT technique must be employed to (1) accurately track the GMPP under any shading conditions, (2) obtain rapid processing time to track the actual GMPP under sudden environmental changes, and (3) perform the tracking process with minimal disruptive oscillations. Moving shadows are the most common rapidly changing environmental conditions, thereby causing substantial disruptions to the stability and efficiency of the PV system. These conditions are often

1551-3203 (c) 2018 IEEE. Personal use is permitted, but republication/redistribution requires IEEE permission. See http://www.ieee.org/publications_standards/publications/rights/index.html for more information.

This article has been accepted for publication in a future issue of this journal, but has not been fully edited. Content may change prior to final publication. Citation information: DOI 10.1109/TII.2019.2895066, IEEE Transactions on Industrial Informatics



typically substantially complex to be created in experimental situations due to the limitations of the experimental test benches. However, the powerful experimental test bench setup used in the current study enabled the creation and use of such conditions for the evaluative analysis of the proposed MPPT technique. To create the scenarios, an array comprising six KC85T PV series-connected modules was designed using Chroma Soft Panel software. A moving shadow was created to enable the modules to receive varying irradiance levels in accordance with the location of the shadow on top of the solar array. A new PS scenario was created after each movement. Overall, the designed PV array experienced 7 shading patterns in a span of approximately 1 min. The MPPT system initiated the tracking process after each change based on the initialization conditions designed for all participating techniques. The final results show that the standard PSO causes many disruptive fluctuations during the tracking period, thereby significantly harming the overall stability of the PV system (see Fig. 12). The negative impact of these problems was modified and addressed in the proposed MPSO method. Nonetheless, the experimental output results show that although the magnitude and frequency of the fluctuations at the output of the PV system have been reduced, the problem remains for the MPSO-based MPPT technique. Apart from the problem of fluctuations, the tracking speed of these techniques, particularly the PSO technique, is extremely long, thereby causing substantial problems when the PV system undergoes rapidly changing conditions. These conditions are extremely common in the application of PV systems in numerous dynamic systems, such as electric vehicles, robotics, or even for residential PV systems, which are in densely populated and busy areas. The output results show that compared with the PSO methods, the convergence speed in the MPSO method is substantially higher, and the particles begin converging after the initial iterations. However, the overall tracking process remains lengthy. To address the aforementioned issues, the proposed ARMO method was evaluated under the first shadow moving condition. With respect to the main criteria for a reliable MPPT system, the ARMO technique accurately tracks GMPP in all shading conditions without any steady-state oscillation at the output terminal of the system (see Fig. 12 (c)). In addition, the experimental results indicate that the tracking process of the proposed MPPT technique is substantially faster, thereby resulting in substantially smooth and dynamic performance under rapidly changing conditions. During the majority of the changes in shading, the ARMO-based MPPT tracks the actual GMPP in approximately 1 s while the tracking times for the other two metaheuristic methods were around 4 s. Furthermore, the magnitude and quantity of the output fluctuations during the tracking periods are substantially reduced when ARMO is used. Apart from the first few fluctuations at the output curves, the ARMO technique immediately converged toward GMPP in a short period. The system has no information on the output characteristics because of the nature of system-independent methods and the unpredictable behavior of PS conditions. Therefore, the initial fluctuations at the output of the PV system are unavoidable because the search space and fitness of the initial particles must be evaluated in the first iterations. The strength of the soft computing and metaheuristic approaches are typically evaluated with respect to convergence speed. This evaluation determines the convergence speed of the participating particles toward global fitness after the initial exploration of the search space.

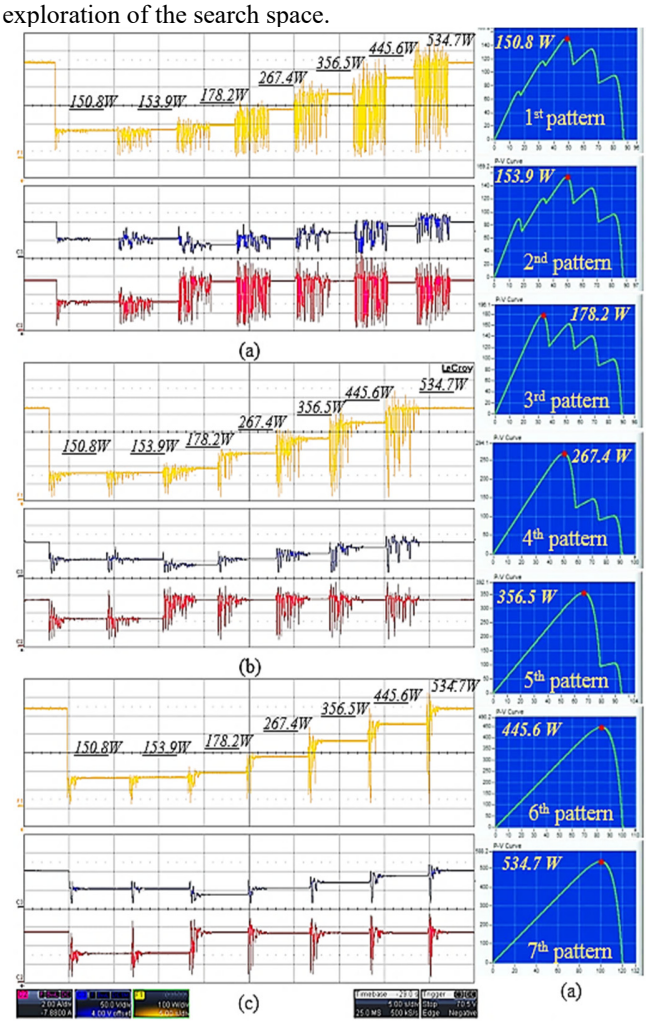


Fig. 12. Experimental comparison of different MPPT techniques under rapidly varying PS conditions: (a) PSO, (b) MPSO, and (c) ARMO methods

### *D. Ramp Change*

Another common type of rapidly changing environmental conditions is the ramp change. This condition occurs when the overall irradiance level changes uniformly in the surroundings of a PV system and occurs frequently in the real world, particularly when large shadows move rapidly on top of the solar arrays. Using the Chroma Soft Panel software, a condition was designed in which the overall solar irradiance increases from 100 to 1000 W/m$^2$ within 1 min. The output results shown in Fig. 13 show that in the majority of the changes, the tracking process of PSO- and MPSO-based MPPT systems exceeds the time taken for solar irradiance to change from one level to another. This process means that the convergence speed of these methods is faster than the pace of change in irradiance levels and before the MPPT converges toward GMPP, the irradiance level changes, and the algorithm is reinitialized. Therefore, significant fluctuations are present at the output of the PV system, as shown in Fig. 13 (a) and (b). Such fluctuations certainly disrupt the reliability and stability of the overall PV system. In Fig. 13 (c), the ARMO-based MPPT not only converges toward GMPP in a very short time (less than 1 s in the majority of the tests) but also cause less fluctuation at the

1551-3203 (c) 2018 IEEE. Personal use is permitted, but republication/redistribution requires IEEE permission. See http://www.ieee.org/publications_standards/publications/rights/index.html for more information.

This article has been accepted for publication in a future issue of this journal, but has not been fully edited. Content may change prior to final publication. Citation information: DOI 10.1109/TII.2019.2895066, IEEE Transactions on Industrial Informatics



output of the PV system, compared with the standard PSO and MPSO methods. Apart from a few initial fluctuations, which are unavoidable and are caused by the initial exploration of the search space, the ARMO–MPPT controller converges promptly toward GMPP.

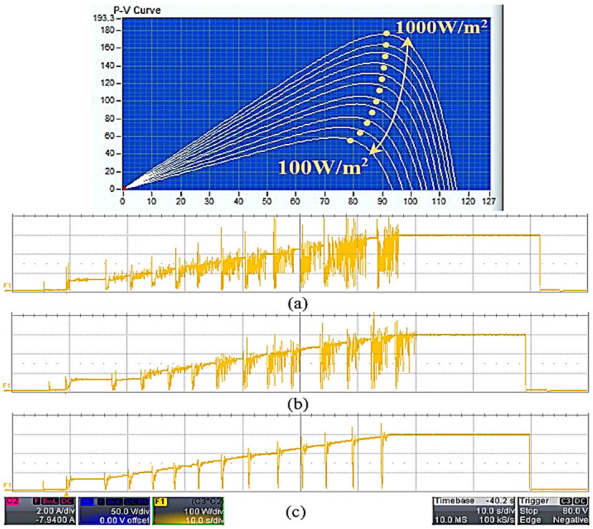


Fig. 13. Experimental comparison of different MPPT techniques under rapidly varying uniform irradiance levels: (a) PSO, (b) MPSO, and (c) ARMO methods

Notably, in many of the applications, such as PV to grid integration, the time limitation for the stability of the system is 2 s. This phenomenon means that the RMO technique can meet the requirements of many PV applications because its total tracking period is < 1.5 s. Thus, the tracking period can be reduced by changing the stopping condition in the MPPT control system. In this project, the completion of a predefined iteration number is selected as the stopping condition. Such a condition requires more time to finalize the output signal of the MPPT controller. In some cases, other stopping conditions, such as a predefined small error or the repletion in the results of multiple iterations in the algorithm, can result in shorter tracking time. Compared with the conventional MPPT techniques, the intelligent approaches commonly have lower oscillation around MPPT and better tracking capability for sudden changes in irradiance levels. However, their behavior with regard to the main criteria, such as efficiency, reliability under PSCs, convergence speed, system independence, and steady-state oscillation, might be different. Table II and Fig. 14 show the comparison between the proposed algorithm and other methods in the literature. The proposed algorithm has higher efficiency than the conventional incremental conductance algorithm because it can track the GMPP accurately most of the time. The InC algorithm is dependent on the initial search location, and it fails to track the GMPP if the initial point is not located in the area that consists of GMPP. In addition, the InC method has a steady-state oscillation that reduces the efficiency of the system. In terms of simplicity in application, the proposed method can be implemented easily compared with other optimization algorithms, such as PSO, MPSO, and Grey Wolf Optimization based MPPT techniques, because the proposed algorithm requires less memory space in the microcontroller as not all the particles in each iteration have to be stored in the memory. The proposed method only needs to store the *Rbest* and *Gbest* to be used in the next iteration. Therefore, the proposed algorithm is easier to implement in the microcontroller with less memory space and requires a simpler program. In addition, the proposed algorithm only requires the tuning of two coefficients compared with the three coefficients in the Grey Wolf method. Thus, the proposed algorithm is easier in tuning and has higher reliability than the Grey Wolf Optimization algorithm. Moreover, the proposed algorithm uses a random initial searching location that reduces the dependency on the selection of the initial location. Meanwhile, the PSO and Grey Wolf Optimization methods use a fix initial location, which increases the possibility of missing the GMPP if the inaccurate initial location is selected. As shown in the experimental results, the proposed algorithm also has lower fluctuation during GMPP tracking; thus, the stability of the system can be significantly increased compared with other methods such as PSO and MPSO. Finally, the tracking speed of the proposed algorithm is faster than that of other methods, such as PSO, as shown in the experimental setup. Thus, the proposed algorithm has better performance with higher efficiency and reliability in implementation. An analytical comparison is presented in Fig 14. In this figure, “A” refers to the reliability of the method under PS conditions, “B" to fluctuations during tracking period, “C” to the simplicity of the method, “D” to convergence/tracking speed, “E” to efficiency and “F” to computational cost.

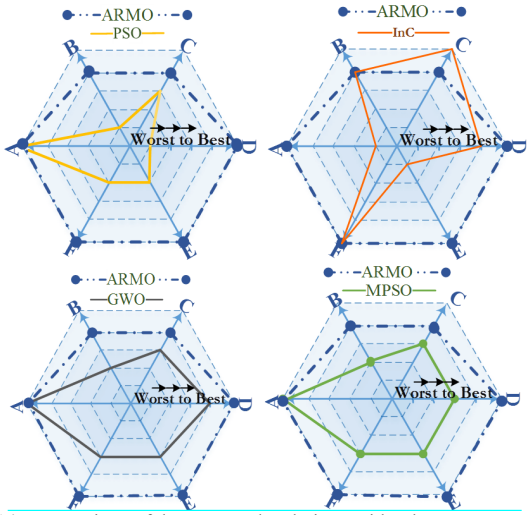


Fig. 14. Comparison of the proposed technique with other MPPT methods according to six main parameters

### *E. Comparison with standard RMO technique*

In contrast to the original RMO presented in reference [26] in the revised manuscript, in the proposed ARMO technique, the values of these coefficients adapt during the algorithm process. In the proposed ARMO method, the values of C1 and C2 are adapted throughout the iterations which helps the proposed algorithm to change the significance of $R_{best}$ and $G_{best}$ parameters throughout the different iterations based on the movement trajectory of the particles. In addition, in the proposed ARMO technique, the value of inertia weight (Wk) decreases faster than the way that has been considered in the original RMO. Furthermore, the value of this coefficient remains constant in the initial iterations, thereby allowing particles to explore the larger sections of the search space in the early stage where the region for GMPP is not yet identified. This faster decrease in the following iteration helps the particles

1551-3203 (c) 2018 IEEE. Personal use is permitted, but republication/redistribution requires IEEE permission. See http://www.ieee.org/publications_standards/publications/rights/index.html for more information.

This article has been accepted for publication in a future issue of this journal, but has not been fully edited. Content may change prior to final publication. Citation information: DOI 10.1109/TII.2019.2895066, IEEE Transactions on Industrial Informatics



converge toward the actual GMPP at the final iterations when the global region is identified. The performance of the ARMO is compared standard RMO technique under partial shading condition and presented in Fig. 15. As shown in the results, the proposed ARMO technique has faster convergence speed, less output fluctuation and more stable tracking compared with standard RMO technique.

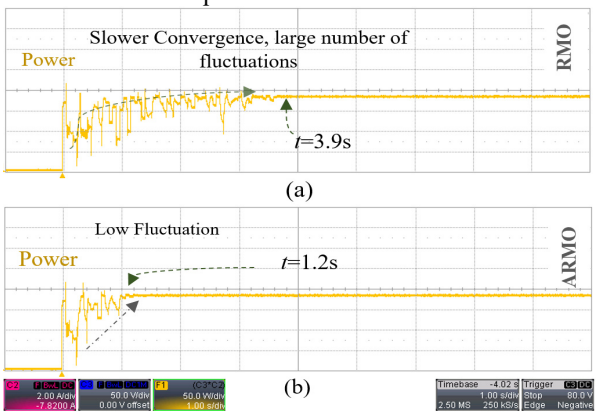


Fig. 15. Experimental comparison of ARMO and RMO under partial shading condition

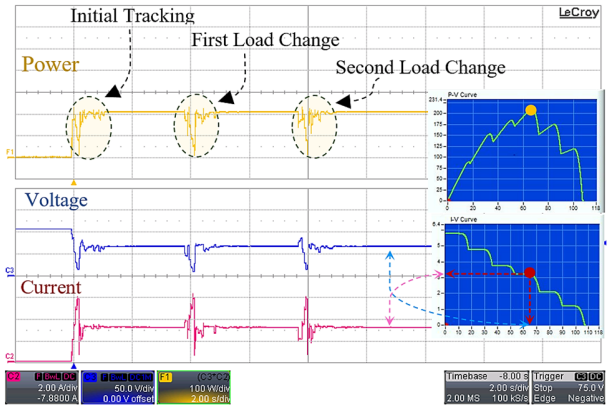


Fig. 16. Experimental results of the proposed ARMO technique under sudden load change condition

### *F. Sudden load changes under partial shading conditions*

In addition to the aforementioned changing irradiance conditions, load variation is another prevalent situation the affects the systems. Thus, the load-varying condition is included in experimental verifications to evaluate the dynamic ability of the proposed technique. In this test, the MPPT techniques are tested for different load levels when the system was operated under PS Scenario 1. Fig. 16 shows that when the controller finds the MPP, the system stabilizes if no change happens. At $t$ = 5.6 s, the load is changed to $R$ = 10 Ω; thus, the controller begins to work. At $t$ = 6.8 s, the MPP stops working by finalizing all iterations and tracking the MPP. At $t$ = 9.6 s, the load is changed to $R$ = 20 Ω, and the controller starts working until it finds the MPP at $t$ = 10.8 s. Changing the output load does not prevent the algorithm from successfully capturing the proper MPP.

## V. Conclusion

The main objective of this study was to develop a new MPPT technique with fast-tracking speed, high reliability, and low output fluctuation for the PV system operating under different PS conditions. A novel rapid, simple, and efficient method called ARMO was designed and developed to track the GMPP at the output of a partially shaded PV system. An extensive experimental implementation was conducted to evaluate the performance of the proposed ARMO technique in a real-world environment. According to the experimental results, the main strengths of the proposed technique are the following: (1) The proposed technique is system-independent due to its stochastic nature. (2) Compared to conventional methods, the proposed ARMO method has high efficiency and reliability in tracking the GMPP under intensive PS conditions. (3) Compared to the standard and modified PSO methods, the proposed method has significantly faster-tracking speed. (4) Compared to the other metaheuristic methods, the proposed method causes much lower fluctuations at the output of the PV system under static and moving PS conditions. (5) Unlike the majority of metaheuristic methods, the ARMO-based MPPT technique does not require a large memory to record the movements of each particle throughout the optimization operation. Therefore, the computational burden within the processing time is reduced and a low-cost microcontroller can be used as the main MPPT controller. The presented experimental implementation provided a unique platform to conduct a fair comparison among different MPPT methods, including the ARMO method, modified and standard PSO methods, and conventional InC method. The results also revealed the following main aspects: (1) importance of GMPP tracking ability under PS conditions; (2) advantages of a metaheuristic approach over conventional MPPT techniques in tracking GMPP under PS conditions; (3) limitations of the standard and modified PSO in terms of output fluctuations and tracking speed under both static and moving PS conditions; and (4) significant improvements to the standard and modified PSO in the new proposed ARMO MPPT techniques. The aforementioned issues and the superiority of the proposed ARMO method over other MPPT techniques were addressed and thoroughly discussed in this study.

TABLE II. COMPARISON OF THE PROPOSED TECHNIQUE WITH OTHER MPPT METHODS

| Evaluated Parameter | InC | PSO – [11, 12] | MPSO (DEPSO)- [19] | Grey Wolf – [22, 23] | RMO [26] | Proposed Method (ARMO) |
|---|---|---|---|---|---|---|
| GMPP tracking capability | No | Yes | Yes | Yes | Yes | Yes |
| Simplicity | Simple | Medium | Medium | Medium | Simple | Simple |
| Efficiency | Low | High | High | High | High | Very High |
| Tracking speed | High | Medium | Medium | Medium | Medium | High |
| Steady-state oscillation | Yes | No | No | No | No | No |
| Initial location dependency | Yes | Yes | No | Yes | No | No |
| Reliability | Low | Medium | Medium | Medium | Medium | High |

1551-3203 (c) 2018 IEEE. Personal use is permitted, but republication/redistribution requires IEEE permission. See http://www.ieee.org/publications_standards/publications/rights/index.html for more information.

This article has been accepted for publication in a future issue of this journal, but has not been fully edited. Content may change prior to final publication. Citation information: DOI 10.1109/TII.2019.2895066, IEEE Transactions on Industrial Informatics



REFERENCES


[1] R. J. Yang and P. X. W. Zou, "Building integrated photovoltaics (BIPV): costs, benefits, risks, barriers and improvement strategy," *International Journal of Construction Management,* vol. 16, no. 1, pp. 39-53, 2016/01/02 2016.

[2] M. Killi and S. Samanta, "An Adaptive Voltage-Sensor-Based MPPT for Photovoltaic Systems With SEPIC Converter Including Steady-State and Drift Analysis," *IEEE Transactions on Industrial Electronics,* vol. 62, no. 12, pp. 7609-7619, 2015.

[3] F. Paz and M. Ordonez, "High-Performance Solar MPPT Using Switching Ripple Identification Based on a Lock-In Amplifier," *IEEE Transactions on Industrial Electronics,* vol. 63, no. 6, pp. 3595-3604, 2016.

[4] S. M. R. Tousi, M. H. Moradi, N. S. Basir, and M. Nemati, "A Function-Based Maximum Power Point Tracking Method for Photovoltaic Systems," *IEEE Transactions on Power Electronics,* vol. 31, no. 3, pp. 2120-2128, 2016.

[5] S. Sajadian and R. Ahmadi, "Model Predictive-Based Maximum Power Point Tracking for Grid-Tied Photovoltaic Applications Using a <italic>Z</italic>-Source Inverter," *IEEE Transactions on Power Electronics,* vol. 31, no. 11, pp. 7611-7620, 2016.

[6] Syafaruddin, E. Karatepe, and T. Hiyama, "Artificial neural network-polar coordinated fuzzy controller based maximum power point tracking control under partially shaded conditions," *Renewable Power Generation, IET,* vol. 3, no. 2, pp. 239-253, 2009.

[7] B. N. Alajmi, K. H. Ahmed, S. J. Finney, and B. W. Williams, "A Maximum Power Point Tracking Technique for Partially Shaded Photovoltaic Systems in Microgrids," *Industrial Electronics, IEEE Transactions on,* vol. 60, no. 4, pp. 1596-1606, 2013.

[8] B. N. Alajmi, K. H. Ahmed, S. J. Finney, and B. W. Williams, "Fuzzy-Logic-Control Approach of a Modified Hill-Climbing Method for Maximum Power Point in Microgrid Standalone Photovoltaic System," *Power Electronics, IEEE Transactions on,* vol. 26, no. 4, pp. 1022-1030, 2011.

[9] S. K. Kollimalla and M. K. Mishra, "Variable perturbation size adaptive P&O MPPT algorithm for sudden changes in irradiance," *IEEE Transactions on Sustainable Energy,* vol. 5, no. 3, pp. 718-728, 2014.

[10] J. Ahmed and Z. Salam, "A Modified P&O Maximum Power Point Tracking Method With Reduced Steady-State Oscillation and Improved Tracking Efficiency," *IEEE Transactions on Sustainable Energy,* vol. 7, no. 4, pp. 1506-1515, 2016.

[11] M. Miyatake, M. Veerachary, F. Toriumi, N. Fujii, and H. Ko, "Maximum Power Point Tracking of Multiple Photovoltaic Arrays: A PSO Approach," *Aerospace and Electronic Systems, IEEE Transactions on,* vol. 47, no. 1, pp. 367-380, 2011.

[12] L. Yi-Hwa, H. Shyh-Ching, H. Jia-Wei, and L. Wen-Cheng, "A Particle Swarm Optimization-Based Maximum Power Point Tracking Algorithm for PV Systems Operating Under Partially Shaded Conditions," *Energy Conversion, IEEE Transactions on,* vol. 27, no. 4, pp. 1027-1035, 2012.

[13] C. Manickam, G. P. Raman, G. R. Raman, S. I. Ganesan, and N. Chilakapati, "Fireworks Enriched P&O Algorithm for GMPPT and Detection of Partial Shading in PV Systems," *IEEE Transactions on Power Electronics,* vol. 32, no. 6, pp. 4432-4443, 2017.

[14] Y. Shaiek, M. Ben Smida, A. Sakly, and M. F. Mimouni, "Comparison between conventional methods and GA approach for maximum power point tracking of shaded solar PV generators," *Solar Energy,* vol. 90, pp. 107-122, 2013.

[15] S. Lyden and M. E. Haque, "A Simulated Annealing Global Maximum Power Point Tracking Approach for PV Modules Under Partial Shading Conditions," *IEEE Transactions on Power Electronics,* vol. 31, no. 6, pp. 4171-4181, 2016.

[16] R. B. A. Koad, A. F. Zobaa, and A. El-Shahat, "A Novel MPPT Algorithm Based on Particle Swarm Optimization for Photovoltaic Systems," *IEEE Transactions on Sustainable Energy,* vol. 8, no. 2, pp. 468-476, 2017.

[17] K. Ishaque and Z. Salam, "A Deterministic Particle Swarm Optimization Maximum Power Point Tracker for Photovoltaic System Under Partial Shading Condition," *Industrial Electronics, IEEE Transactions on,* vol. 60, no. 8, pp. 3195-3206, 2013.

[18] K. L. Lian, J. H. Jhang, and I. S. Tian, "A Maximum Power Point Tracking Method Based on Perturb-and-Observe Combined With Particle Swarm Optimization," *Photovoltaics, IEEE Journal of,* vol. 4, no. 2, pp. 626-633, 2014.

[19] M. Seyedmahmoudian *et al.*, "Simulation and Hardware Implementation of New Maximum Power Point Tracking Technique for Partially Shaded PV System Using Hybrid DEPSO Method," *Sustainable Energy, IEEE Transactions on,* vol. 6, no. 3, pp. 850-862, 2015.

[20] C. Manickam, G. R. Raman, G. P. Raman, S. I. Ganesan, and C. Nagamani, "A Hybrid Algorithm for Tracking of GMPP Based on P&O and PSO With Reduced Power Oscillation in String Inverters," *IEEE Transactions on Industrial Electronics,* vol. 63, no. 10, pp. 6097-6106, 2016.

[21] S. Mohanty, B. Subudhi, and P. K. Ray, "A new MPPT design using grey wolf optimization technique for photovoltaic system under partial shading conditions," *IEEE Transactions on Sustainable Energy,* vol. 7, no. 1, pp. 181-188, 2016.

[22] N. Kumar, I. Hussain, B. Singh, and B. Panigrahi, "Rapid MPPT for Uniformly and Partial Shaded PV System by using JayaDE Algorithm in Highly Fluctuating Atmospheric Conditions," *IEEE Transactions on Industrial Informatics,* 2017.

[23] S. Mohanty, B. Subudhi, and P. K. Ray, "A Grey Wolf-Assisted Perturb & Observe MPPT Algorithm for a PV System," *IEEE Transactions on Energy Conversion,* vol. 32, no. 1, pp. 340-347, 2017.

[24] M. Seyedmahmoudian, S. Mekhilef, R. Rahmani, R. Yusof, and E. T. Renani, "Analytical modeling of partially shaded photovoltaic systems," *Energies,* vol. 6, no. 1, pp. 128-144, 2013.

[25] R. Rahmani and R. Yusof, "A new simple, fast and efficient algorithm for global optimization over continuous search-space problems: Radial Movement Optimization," *Applied Mathematics and Computation,* vol. 248, pp. 287-300, 12/1/ 2014.

[26] M. Seyedmahmoudian, B. Horan, R. Rahmani, A. Maung Than Oo, and A. Stojcevski, "Efficient Photovoltaic System Maximum Power Point Tracking Using a New Technique," *Energies,* vol. 9, no. 3, p. 147, 2016.


**Mehdi Seyedmahmoudian** (M'11) is the Senior Lecturer School of Software & Electrical Engineering at Swinburne University of Technology, Australia. He holds B.Sc. degree, M. Eng. Degree and PhD degree in Electrical Engineering. His research interests includes renewable Energy systems, smart grids and Microgrid systems and the application of emerging technologies in Green renewable Energy Development.

**Kok Soon Tey** (M'15) received the B. Eng. (Hons.) and Ph.D. degrees in electrical engineering from the University of Malaya, Kuala Lumpur, Malaysia, in 2011 and 2014 respectively. He is currently a Senior Lecturer in the Department of Computer System and Technology. His research interests include control of converters, power efficiency of photovoltaic (PV) system, inverter control of PV system and embedded system design.

**Ben Horan** received the B. Eng (Hons.) and Ph.D. in Engineering from Deakin University in 2005 and 2009 respectively. He is currently Associate Professor and Associate Head of School-research and Director of the CADET VR Lab within the School of Engineering, Deakin University, Australia. His cresearch interests include mechatronics, virtual reality and renewable energy.

**Alireza Safdari Ghandhari** is currently a project manager at CRAE TECH. His work is mainly focused on embedded systems and product development for robotic related industries and applications.He is also working closely with Center of Research in Applied Electronics directed by Prof. Dr. Mahmoud Moghavvemi at University of Malaya, Kuala Lumpur, Malaysia. He collaborates with the center on development of medical devices.

**Saad Mekhilef** (M'01-SM'12) is an IET Fellow and IEEE senior member. He is the associate editor of IEEE Transaction on Power Electronics and Journal of Power Electronics. He is currently a Professor in the Department of Electrical Engineering, University of Malaya and Director of Power Electronics and Renewable Energy Research Laboratory- PEARL. He is the author and co-author of around 250 publications in international journals and proceedings. His research interests include power conversion techniques, control of power converters, renewable energy and energy efficiency.

**Alex Stojcevski** is the Dean of School of Software & Electrical Engineering at Swinburne University of Technology, Melbourne Australia. Alex holds a PhD degree, Masters by research degree in Electrical and Electronics Engineering, and a Bachelor degree in Electrical Engineering. He has held numerous senior positions in several universities across different countries. Professor Stojcevski's research interests are in renewable energy and micro grid design. He has published more than 250 book chapters, journals, and conference articles and has given a number of internationally invited speaker presentations.

1551-3203 (c) 2018 IEEE. Personal use is permitted, but republication/redistribution requires IEEE permission. See http://www.ieee.org/publications_standards/publications/rights/index.html for more information.